

# Atlas-based 3D-Shape Reconstruction from X-Ray Images

Hans Lamecker\*, Thomas H. Wenckeback, Hans-Christian Hege  
Zuse Institute Berlin - Visualization and Data Analysis  
Takustr. 7, 14195 Berlin, Germany  
{lastname}@zib.de

## Abstract

*In many cases x-ray images are the only basis for surgery planning. Nevertheless it is desirable to draw conclusions about the 3D-anatomy of the patient from such data. This work presents a method to reconstruct 3D shapes from few digital x-ray images on the basis of 3D-statistical shape models. At the core of this method lies an algorithm which optimizes a similarity measure assessing the difference between projections of the shape model and the x-ray images. Based on theoretical and experimental observations we propose to measure the distance between the silhouettes of the object in the projections. The method is tested on 23 synthetically generated x-rays from CT data sets of the geometrically as well as topologically complex shape of the pelvic bone.*

## 1. Motivation

X-ray images still play a crucial role in diagnosis and surgery or therapy planning. Accurate computer-aided pre-operative planning, however, requires the knowledge of the 3D-geometry of the anatomy. The problem addressed in this work is how to reconstruct the a-priori unknown 3D-geometry of objects from 2D-projection images.

One of the most prominent applications is the treatment of degenerative joint diseases by artificial hip joint replacement. A large number of hip prostheses are implanted per year. Due to the aging of the population a strong rise in this number is expected for the future. While it is known that the loads on the hip joint play a crucial role for the long-term function and successful performance of artificial joints, there exists no reliable data about expected joint loads for surgical planning. Computer-assisted planning shall help to further improve the treatment in order to as-

<sup>1</sup>Hans Lamecker is supported by the DFG Research Center MATHEON "Mathematics for Key Technologies" in Berlin. The authors thank O. Etmuss for first experiments and implementations, M. Heller, G. Duda, A. Sharenkov for fruitful discussions and J. Schröder for x-ray images.

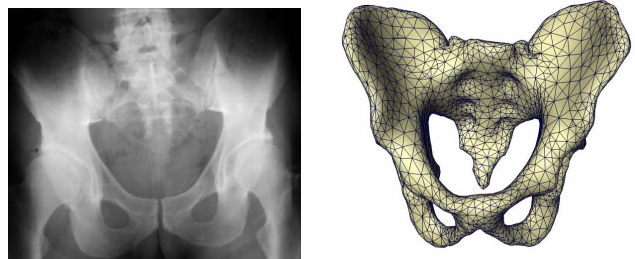


Figure 1. 3D-reconstruction from x-ray

sure an individual and optimal biomechanical reconstruction of the hip. To this end, arising forces and loads before and after the intervention shall be computed via validated biomechanical models. Most commonly, the basis for such simulations are x-ray images. While substantial data for the adjustment of biomechanical model parameters can be extracted from coronal x-ray images [3], a more accurate analysis of the loads requires the knowledge of the 3D-geometry of the bone and muscles.

## 2. Previous Work

A large portion of the work concerning 2D/3D-registration (cf. van de Kraats et al. [10] and references therein) is based on the assumption that there exists pre-operative 3D-data of the patient, which shall be registered to data acquired intra- or post-operatively. This work however addresses the problem of reconstructing 3D-objects from 2D-data, where no such reference is available. Among many differently parameterized deformable surface models (see Montagnat et al. [5] for an overview), models that incorporate a-priori knowledge about typical shape variations occurring in the object to be reconstructed seem to be most suitable for this task due to their robustness. Miscellaneous works build upon this idea:

Fleute et al. [2] use a 3D-statistical shape model of the distal femur for registration with x-ray images from a C-arm. They minimize the distances between the contours of the

model surface and the contours formed by a discrete number of projections rays within the x-ray acquisition setting using the ICP algorithm. Benameur et al. [1] build and use a 3D-statistical shape model of vertebrae for registration and segmentation of x-ray images. The registration consists of a minimization of an image edge potential, which measures the distance of the projected contours to the contours in the x-ray images. Yang et al. [8] generate a hybrid shape model for the reconstruction of femurs from x-ray data. The correlation between simulated thickness images of the shape model and the x-ray images serves as the similarity measure for the optimization.

In contrast to the previous work we propose to measure the distance between the model and the data based on their silhouettes. We validate our method using synthetically generated x-ray images from CT data of the pelvic bone.

### 3. Methods

#### 3.1. Statistical Shape Model

The shape model used in this work is generated from a set of individual training shapes (triangulated surfaces). The main challenge lies in the correct identification of anatomically corresponding points on each training surface. The method described by Lamecker et al. [4] was adopted to generate the shape model of the pelvis, but a variety of other approaches exists, too. In this method each training shape is decomposed into a number of corresponding regions interactively. Each of these regions is then mapped consistently to a common base domain under the constraint of minimizing metric distortion. Concatenating these parameterizations directly yields the desired correspondence map. As a result of this process, all training shapes  $\mathbf{v}_i$  ( $i = 1, \dots, n$ ) can be represented in a common vector space of dimension  $3m$ , with  $m$  the number of sample points used to discretize the shapes (vertices of the surfaces). Principal component analysis (PCA) on this set of vectors provides a compact representation of the variability within the training set, resulting in a bilinear model:

$$\mathcal{S}(\mathbf{b}, T) = T \left( \bar{\mathbf{v}} + \sum_{k=1}^n b_k \mathbf{p}_k \right)$$

where  $\bar{\mathbf{v}} = \sum \mathbf{v}_i / n$  is the average shape,  $\mathbf{p}_k$  the eigenmodes of the covariance matrix  $C = \sum (\mathbf{v}_i - \bar{\mathbf{v}})(\mathbf{v}_i - \bar{\mathbf{v}})^T / n$ . The shape weights  $\mathbf{b}$  and the linear transformation  $T$  constitute the degrees of freedom of the model.

#### 3.2. Thickness of the Shape Model

For a given camera calibration  $K$  (location and orientation of the x-ray source w.r.t. the image acquisition planes)

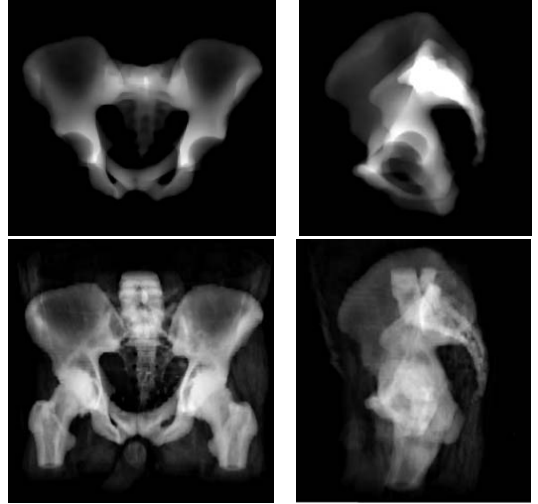


**Figure 2.** *top*: thickness images (projected shape model), *bottom*: simulated x-ray images

and a given instance of the shape model  $\mathcal{S}(\mathbf{b}, T)$ , a thickness image of the shape model in the image acquisition plane is computed by computing the propagation length of simulated rays through the volume enclosed by the shape model (Fig. 2, top). This can efficiently be accomplished using graphics hardware acceleration.

#### 3.3. Simulated X-Ray

In order to illustrate the reasoning for the choice of the similarity measure in this work, synthetic x-ray images are generated from CT-data sets using the volume rendering technique. Such artificial data possesses a high degree of realism [6] (Fig. 2, bottom). Besides, the same CT-data sets were used to extract the training set for the statistical shape model, and will later be used for evaluating the method. Hence we are able to directly compare projection data of the shape model with calibrated x-ray images.

#### 3.4. Silhouette Extraction

From both the thickness and the simulated x-ray images accentuated contours are extracted using a Canny [8] edge detector (Fig. 3). Finally, the silhouette is extracted from the projection images. The silhouette can automatically be computed from the thickness images: it is its zero level-set, i.e. it separates pixels with thickness  $> 0$  from pixels with thickness  $= 0$ . However, the silhouette must be determined interactively in the x-ray images: wrong edges are discarded or missing edges are added to the silhouette (demonstrated in Fig. 4 on real x-ray images). The final contours are rasterized as 2D-images.



**Figure 3. Canny edge maps.** *top row: thickness, bottom row: simulated x-ray images*

### 3.5. Choice of Similarity Measure

The desired 3D-reconstruction is given by the solution of the optimization problem  $\mathbf{x}^* = \arg \min_{\mathbf{x}} D(\mathbf{x})$  where  $D(\mathbf{x})$  with  $\mathbf{x} = (\mathbf{b}, T, K)$  measures the dissimilarity between a projected shape model instance and a set of x-ray images.

**Approach 1:** The most obvious and fully automatic choice for  $D$  would be an intensity correlation between the thickness and the x-ray image (cf. Tang et al. [8]), e.g. by sum of squared differences or mutual information. However, our experiments showed unsatisfactory results on the pelvic data. The approach produces mismatches on the inside of the pelvis since it does not take into account inhomogeneities there (Fig. 2). Another cause for problems is the additional structure that is present on the outside in the x-ray data but not in the thickness image.

**Approach 2:** The second most obvious choice consists in measuring the distance between the edge-maps (cf. Be-



**Figure 4. Left: Canny edge detection in x-ray, Right: silhouette in the x-ray.**

nameur et al. [1]). This approach is almost automatic, as it involves adjusting some parameters of the Canny-filter. Let

$$d(\mathbf{x}, s') = \min_{\mathbf{x}' \in s'} \|\mathbf{x} - \mathbf{x}'\|$$

be the distance between a point  $\mathbf{x}$  in the set of contour  $s$  of the thickness image and the set of contours  $s'$  of the x-ray image. Then

$$D = \int_{\mathbf{x} \in s} d(\mathbf{x}, s')^2 dx + \int_{\mathbf{x} \in s'} d(\mathbf{x}, s)^2 dx.$$

In order to efficiently evaluate this distance, the distance map of both the model and the x-ray contours are computed.

**Our approach:** However, considering the full edge-maps failed to produce acceptable results, due to the fact many contours have no well-defined corresponding counterpart (see Fig. 3). Hence we propose to consider the silhouettes of the objects instead of the full edge-maps  $s$  and  $s'$  (Fig. 4), which alleviates the problems mentioned.

## 4. Optimization

The distance function  $D$  is non-linear and generally exhibits many local minima. Thus, we use a gradient-descent evolution for the minimization of  $D$ :  $\dot{\mathbf{x}}(t) = -\nabla D(\mathbf{x})$  with some initial value  $\mathbf{x}(0) = (\mathbf{b}_0, T_0, K_0)$ . We replace the gradient  $\nabla D$  by a more suitable search direction, which is computed via a method that evaluates the distance measure at the bounds of a large interval, hence avoiding the solution from being stuck in local minima. In addition, a multi-resolution approach is adopted by performing the registration in a data pyramid: the silhouettes are considered at different resolutions during the course of the optimization. This also speeds up the computation time considerably [7].

## 5. Experiments

For validation of the proposed method 23 CT data sets of the abdomen without bone defects were used (resolution  $1 \times 1 \times 5$  mm). For all data sets manual segmentations of the pelvic bone were available as a gold standard for quantitative evaluation. The statistical shape model was generated from triangulated surfaces reconstructed from the manual segmentations [4].

The goal of this evaluation is to examine the accuracy achievable with the proposed method. The main ingredients of this method to be tested are the statistical shape model and the similarity measure. Therefore we assume that the camera calibration  $K$  and the linear transformation  $T$  is known and need not be optimized. For evaluation purposes these parameters are known from the generation of the simulated x-ray images. In fact these assumptions often

| Test       | Mean [mm] | Median [mm] | Max [mm]   |
|------------|-----------|-------------|------------|
| LI (CO)    | 1,5 ± 0,5 | 1,2 ± 0,3   | 8,8 ± 3,3  |
| LI (CO-SA) | 1,3 ± 0,5 | 1,1 ± 0,5   | 7,9 ± 2,6  |
| LO (CO)    | 2,6 ± 0,4 | 2,1 ± 0,3   | 17,6 ± 6,5 |
| LO (CO-SA) | 2,4 ± 0,4 | 2,0 ± 0,3   | 14,9 ± 3,1 |
| SO         | 2,0 ± 0,2 | 1,6 ± 0,2   | 13,3 ± 2,6 |

**Table 1. Experimental results (mean values and standard deviations across 23 data sets)**

are met in real world: in conventional surgical planning calibrated x-ray images can be generated under standardized acquisition conditions [9].

All experiments were conducted for one x-ray image (coronal: CO) and two x-ray images (CO plus sagittal: CO-SA). The error was measured by computing the symmetric mean surface distances between optimization result and gold standard. Three different experiments were performed:

(a) *Leave-All-In Test (LI)*: As a test of the similarity measure and the optimization strategy to capture the true 3D-shape, the reconstruction was carried out with a statistical shape model that contained the shape to be reconstructed. The error should ideally reduce to zero.

(b) *Leave-One-Out Test (LO)*: The shape to be reconstructed was removed from the shape model. This represents the “real-world” situation.

(c) *Surface-Optimization (SO)*: As a reference value for the leave-one-out test the shape model was directly matched to the gold standard surfaces in leave-one-out test, where the surface distance between the two shapes was directly minimized [4]. This yields the optimal result to be achieved with a given statistical shape model in the *Leave-One-Out Test* (b). The results are summarized in Table 1.

## 6. Discussion

In this work a new method for the reconstruction of unknown 3D-shapes from x-ray images was presented. The method was validated based on synthetic x-ray data (from pelvic CT) with known camera calibration. The mean values of the measured errors even for a single projection image (coronal) were up to a few millimeters within a range where one can expect to obtain a sufficient estimate of the 3D-geometry with respect to the application of computing load conditions for biomechanical studies [3]. This shall be validated on clinical data in the future. For a complete analysis of the loads occurring in the context of artificial hip joint replacements the method shall be extended to include the femur in a next step. The leave-one-out test shows that the largest portion of the error stems from the incom-

pleteness of the statistical model. Hence the model shall be enlarged by more training data sets in the future. For the clinical application of the method it must be examined to what extent the method can cope with occlusions, artefacts in the x-ray image or pathological situations, e.g. such as degenerative changes of the pelvic bone (adjacent image).



To this end it must be investigated if the method yields sufficient results in cases of incomplete silhouette information. A potential increase in accuracy consists in incorporating further information from the x-ray data and the shape model into the similarity measure for the registration. Hence future work shall attempt to combine silhouette information with modified thickness images into the registration process.

## References

- [1] S. Benameur, M. Mignotte, S. Parent, et al. 3D/2D registration and segmentation of scoliotic vertebrae using statistical models. *Computerized Medical Imaging and Graphics*, 27(5):321–337, 2003.
- [2] M. Fleute and S. Lavalley. Nonrigid 3-d/2-d registration of images using statistical models. In *Proc. MICCAI*, volume 1679, pages 138–147, 1999.
- [3] M. Heller, G. Bergmann, G. Deuretzbacher, et al. Musculoskeletal loading conditions at the hip during walking and stair climbing. *J Biomech*, 34(7):883–893, 2001.
- [4] H. Lamecker, M. Seebaß, H.-C. Hege, and P. Deuffhard. A 3d statistical shape model of the pelvic bone for segmentation. In *Proc. SPIE Medical Imaging: Image Processing*, volume 5370, pages 1341–1351, 2004.
- [5] J. Montagnat, H. Delingette, and N. Ayache. A review of deformable surfaces: topology, geometry and deformation. *Image and Vision Computing*, 19(14):1023–1040, 2001.
- [6] M. Muniyandi, S. Colin, M. Srinivasan, and S. Dawson. Real-time pc based x-ray simulation for interventional radiology training. In *MMVR*, volume 94, pages 233–239, 2003.
- [7] D. Rueckert. Non-rigid registration: Techniques and applications. In J. V. Hajnal, D. L. G. Hill, and D. J. Hawkes, editors, *Medical Image Registration*. CRC Press, 2001.
- [8] T. S. Tang and R. E. Ellis. 2d/3d deformable registration using a hybrid atlas. In *Proc. MICCAI*, volume 3750, pages 223–230, 2005.
- [9] B. The, R. Diercks, R. Stewart, et al. Digital correction of magnification in pelvic x rays for preoperative planning of hip joint replacements: theoretical development and clinical results... *Med Phys*, 32(8):2580–2589, 2005.
- [10] E. van de Kraats, G. Penney, et al. Standardized Evaluation Methodology for 2D-3D Registration. *IEEE Trans Med Imaging*, 24(9):1177–1190, 2005.